Large Amplitude Twisting Motions of an Interdomain Hinge: A Disulfide Trapping Study of the Galactose-Glucose Binding Protein[†]

Claire L, Careaga, Jesse Sutherland, Jilla Sabeti, and Joseph J. Falke*

Department of Chemistry and Biochemistry, University of Colorado, Boulder, Colorado 80309-0215

Received September 16, 1994; Revised Manuscript Received December 14, 1994[®]

ABSTRACT: The galactose–glucose binding protein possesses two structural domains bordering a ligand binding cleft, with three polypeptide strands serving as a flexible hinge connecting the two domains. The hinge is known to bend, enabling the cleft to open by an angle of at least 18°. Here the twisting motions of the hinge were examined by placing pairs of engineered cysteines on the perimeter of the cleft to generate six stable di-cysteine proteins. Each cysteine pair introduced reactive sulfhydryls into both rims of the cleft, one in the N-terminal domain and the other in the C-terminal domain. Collisions between sulfhydryls in different domains were trapped by disulfide formation, yielding sensitive detection of large amplitude domain rotations. When the cleft was occupied by the ligand D-glucose, counterclockwise hinge twist rotations were detected with amplitudes up to 36°, and frequencies ranging from 10^1 to 10^3 collisions s^{-1}. Removal of ligand from the cleft increased the range of twist angles 3-fold and the frequency of motions up to 10^2-fold. Thus, in this representative hinged cleft protein, large amplitude hinge twist motions occur on biologically relevant timescales. The functional implications of such motions are discussed.

The *Escherichia coli* galactose–glucose binding protein (GGBP, 32 kDa) belongs to a diverse group of proteins including a variety of lysozymes, metabolic enzymes, kinases, nucleic acid binding proteins, and small molecule binding proteins which trap substrate in a hinged cleft between two domains [Quiocho et al., 1987; reviewed in Bennett and Huber (1984), Lesk and Chothia (1984), Luck and Falke (1991a) and Gerstein et al. (1994)]. This binding mechanism enables an enzyme to sequester its substrate in a chemically controlled environment or allows a receptor to retain its ligand for an extended period of time, since the time scale of dissociation is controlled by the frequency of cleft opening.

Crystallographic studies have probed key features of hinged cleft movements in several proteins [catabolite gene activator protein (Weber & Steitz, 1987), T4 lysozyme (Dixon et al., 1992), maltose binding protein (Sharff et al., 1992), lysine/arginine/ornithine binding protein (Oh et al., 1993), glutamate dehydrogenase (Stillman et al., 1993), lactoferrin (Gerstein et al., 1993), cAMP-dependent protein kinase, Karlsson et al. (1993), and adenylate kinase (Berry et al., 1994); reviewed by Lesk and Chothia (1994)]. In the simplest cases, the motions of a hinged cleft can be deconvoluted into independent rotations about two orthogonal axes: (i) the hinge-bending rotation yields motion about an axis perpendicular to the interdomain hinge, thereby generating cleft opening and closure, while (ii) the hinge-twisting rotation produces motion about an axis parallel to the hinge, thereby allowing the two surfaces of the cleft to slide relative to one another. In lysozyme, for example, hinge-bending angles ranging from 0° to 32° have been detected in different crystal environments (Faber & Matthews, 1990), while in the maltose binding protein a 35° hinge bend is coupled to

an 8° hinge twisting motion (Sharff et al., 1992). It should be noted, however, that motions of protein domains about a flexible hinge are likely to be perturbed or constrained by crystal packing forces. It follows that hinge motions in solution may have different characteristics, including larger amplitudes, than those observed in crystals.

The galactose and glucose binding protein is a suitable model system in which to examine the amplitudes and frequencies of cleft motions in solution. The structure of the cleft has been defined by X-ray crystallography, although only the closed conformation has been described (Vyas et al., 1987; Zou et al., 1993). Solution NMR studies have placed a lower limit on the hinge bending motion, indicating that the sugar binding cleft can open ≥18° (Luck & Falke, 1991a). The present study examines the hinge-twist motions of the cleft using the disulfide trapping approach (Falke & Koshland, 1987; Careaga & Falke, 1992a,b), which previously revealed the range and frequency of α-helix motions on the protein surface (Careaga & Falke, 1992b). To probe the hinge-twist motion, six different galactose binding proteins have been designed, each possessing a pair of engineered cysteine residues on the edges of its sugar binding cleft. One cysteine is always located at position 182 on the rim of the C-terminal domain, while the second cysteine is positioned on the edge of the N-terminal domain (Figure 1). The resulting engineered proteins, which are stable and active in *in vitro* assays, enable a 142° range of hinge-twist angles to be probed by disulfide bond formation between colliding cysteines on the two domains. The cleft occupied by D-glucose exhibits surprisingly large hinge-twist amplitudes, with frequencies that decrease as the hinge-twist angle, Θ_T, increases. When sugar is removed, the apo-cleft exhibits even larger, more rapid twisting motions. Interestingly, the cleft motion appears to strongly favor one twist-angle direction. Implications for the function of this and other hinged-cleft proteins are discussed.

* Author to whom correspondence should be addressed.
® Abstract published in *Advance ACS Abstracts*, February 1, 1995.

MATERIALS AND METHODS

Generation of Di-Cysteine Engineered Galactose Binding Proteins. The techniques used to engineer and isolate di-cysteine containing galactose binding protein (GGBP) have been described in detail elsewhere (Careaga & Falke, 1992b). Briefly, the plasmid pSF5 (Careaga & Falke, 1992b) was used to generate single-stranded uracil-labeled template DNA for use in site-directed mutagenesis experiments using the selection method of Kunkel (Kunkel et al., 1988; reagents from Bio-Rad Laboratories). In the present study, single-stranded U-labeled DNA containing the M182C mutation was prepared and used as the template in DNA synthesis reactions primed by a mutagenic oligonucleotide, 19 bases in length, which coded for the second cysteine substitution. Following mutagenesis, GGBP genes containing the desired mutations were identified by DNA sequencing as previously described (Careaga & Falke, 1992b).

Di-cysteine-containing GGBP molecules were overproduced by expression of engineered pSF5 in NM303, a strain that lacks endogenous GGBP (Muller et al., 1985). The resulting GGBP protein was isolated, its sugar removed (only for studies of the apo-protein), and stored as described previously (Careaga & Falke, 1992b).

Disulfide Bond Formation and Quantitation. Engineered cysteines were oxidized to disulfides using ambient dissolved O_2 as the oxidant in a reaction triggered by the addition of the redox catalyst 1.5 mM Cu(II)(1,10-phenanthroline)$_3$ (Kobashi, 1968; Careaga & Falke, 1992b). All reactions were carried out at 37 °C in the following reaction buffer: 20 mM NaH_2PO_4, 50 mM NaCl, 50 mM KCl, 1.0 mM D-glucose (where indicated, to maintain saturation of the sugar binding site), 0.2 mM $CaCl_2$ (to maintain saturation of the Ca^{2+} binding site), and 1.0 mM $NaAsO_2$ (to complex residual dithioerythritol; Zahler & Cleland, 1968), pH 7.0 (with NaOH).

Due to the low receptor concentration (2−4 μM), essentially all of the observed disulfide bonded product was intramolecular. At appropriate time points, aliquots were removed and quenched (Careaga & Falke, 1992b), and the products were separated using a modified Laemmli SDS/polyacrylamide gel electrophoresis system containing 15% (w/v) acrylamide, 0.075% (w/v) bisacrylamide, 3.6 M urea, and 10% glycerol (Laemmli, 1970). Gels were stained with Coomassie Brilliant Blue R-250, and then bands were quantitated using laser densitometry as previously described (Careaga & Falke, 1992b). Disulfide-containing GGBP molecules were observed to migrate faster than the wild-type protein; in all cases, treatment of the oxidized protein with excess dithiothreitol for 3 min at 95 °C restored native mobility, verifying that changes in migration were due to intrachain disulfide bonds.

The oxidation reaction yielded not only disulfide formation but also higher oxidation products of cysteine (sulfinic and sulfonic acids), as previously discussed (Careaga & Falke, 1992b). The rate constants of the disulfide reaction and the competing reaction were determined by nonlinear least-squares best fit of the reaction time courses to a two-component rate equation (Careaga & Falke, 1992b). Independently, reactions were carried out to test the intrinsic reactivity of each engineered cysteine with [^{14}C]iodoacetamide using the previously described procedure (Careaga & Falke, 1992b).

Assays for Native Structure and Activity. The three parameters used to check the structure and activity of the di-cysteine GBP molecules were (i) the equilibrium dissociation constant (K_D) for D-galactose binding, measured by fluorescence titration, (ii) the dissociation rate constant (k_d) of Tb^{3+}, measured by a fluorescence assay, and (iii) the ^{19}F NMR spectrum of the 5-fluorotryptophan-labeled protein. All assays were performed as described previously (Careaga & Falke, 1992b).

RESULTS

Choice of Positions for Cysteine Substitution. The six pairs of cysteines engineered to trap hinge-twist motions (Figure 1) were placed along the cleft perimeter at surface locations, thereby minimizing structural perturbations while providing high accessibility to oxidation chemistry. The specific pairs chosen all shared C182 as the probe cysteine, in combination with a second cysteine at the 13, 15, 26, 43, 71, or 95 position. Each of these engineered cysteines was located in a tight turn linking a β-strand to an α-helix at one edge of the cleft, with the exception of C26, located on the surface of an α-helix. Also constructed was a control protein containing the C182 probe in combination with C240, both in the C-terminal domain. The latter protein was designed to test for global unfolding of the C-terminal domain, which would be required to yield disulfide-trapped collisions between these two cysteines lying 18.4 Å apart in the folded domain.

To estimate the hinge-twist angle required for collision of a given pair of cysteines, it was necessary to define the long axis of the hinge connecting the two domains, which would serve as the vertex of the hinge-twisting motion. The approach used to position this axis is illustrated in Figure 2. Briefly, the hinge region consists of three polypeptide segments containing the following residues: hinge strand 1 (G109, T110, D111); hinge strand 2 (L255, N256, D257); and hinge strand 3 (V293, P294, Y295). These residues define three planes approximately parallel to the cleft (Figure 2), such that a given plane contains the α-carbon atom of one residue from each strand: plane 1 (D111, L255, Y295); plane 2 (T110, N256; P294); and plane 3 (G109, D257, V293). A center of mass for the three α-carbons in each plane was calculated, providing three unique points in space. The best-fit line connecting these centers of mass provided the location of the hinge long-axis, as well as the vertex of the hinge-twist angle. This twist angle represented an idealized rotation predicted to bring two engineered cysteines into proximity. Real cysteine−cysteine collisions would typically involve smaller bending motions of the hinge or local motions of the cysteines as well, but for simplicity only the hinge-twist was considered.

Given this definition for the hinge-twist motion, the selected cysteine pairs probed a 142° range of rotational angles. Looking down the long-axis from the N-terminal domain toward the C-terminal domain, the α-carbon of the C182 probe position was virtually superimposed on the α-carbon of C43, defining the zero angle of hinge twisting. The C13, C15, and C26 positions were accessed by counterclockwise hinge twists (−27°, −36°, and −80°, respectively), while C71 and C95 were reached by clockwise twisting (+40° and +62°, respectively). The minimum twist angles and spatial separations of the cysteine pairs are summarized in Table 1.
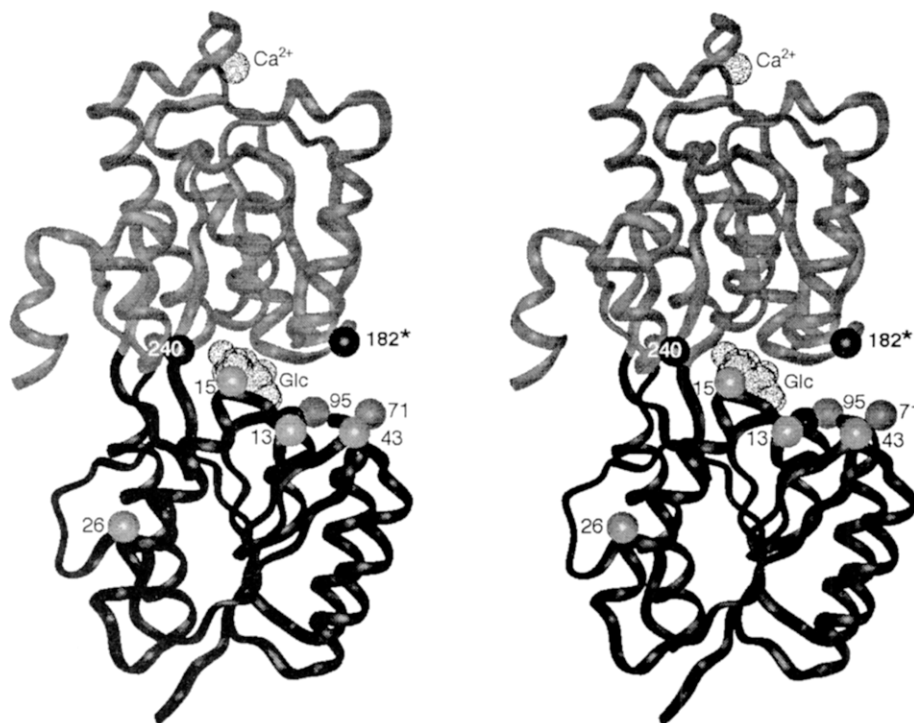
FIGURE 1: Engineered cysteine locations in the structure of the galactose and glucose binding protein. Stereo backbone structure (Vyas et al., 1987) of the binding protein illustrating the distinct N-terminal and C-terminal domains (black and gray ribbons), the ligand D-glucose bound in the cleft between the two domains (dot VDW surface), and the binding site for Ca^{2+} ion (dot VDW sphere). Engineered cysteine locations are indicated by their β-carbon atoms (solid VDW spheres), with the probe position 182 common to all cysteine pairs highlighted (asterisk).

The solvent exposure of each engineered position was also investigated, since this parameter largely determined the accessibility to collisions with other cysteines and to the oxidation agent. Solvent exposures were calculated using the following operational definition: the native side chain in the crystal structure was truncated to its β-carbon, and then the solvent-accessible surface area of this atom was determined (Richards, 1977). All of the engineered cysteine positions exhibited significant solvent exposure, as summarized in Table 1, although a 3-fold range of exposures was observed. Least exposed was the β-carbon of position 15 (28 Å^2), while position 71 possessed the most exposed β-carbon (88 Å^2).

Production of Engineered Galactose Binding Proteins. The GGBP gene was engineered using oligonucleotide-directed mutagenesis, and then overexpressed in an *E. coli* strain lacking the native protein. The purified protein was isolated by standard procedures described under Materials and Methods (Careaga & Falke, 1992b). Oxidation of each di-cysteine protein in the presence of 8 M urea to unfold the protein yielded ≥85% intramolecular disulfide bond formation, verifying the integrity of the engineered cysteines.

Effect of Engineered Cysteines on Protein Integrity. Because the goal of this work was to probe backbone dynamics in the stably folded GGBP structure, it was important to identify the perturbations, if any, generated by the engineered cysteines. Three parameters were measured to quantify the effects of engineered cysteines: (i) the affinity of the sugar binding cleft for D-galactose; (ii) the rate constant for Tb^{3+} dissociation from the calcium binding site; and (iii) the ^{19}F NMR spectrum of the 5-fluorotryptophan labeled protein. Tables 2 and 3 summarize the results of these analyses for the wild-type and seven different di-cysteine GBP molecules.

The affinity of the sugar binding cleft for its ligand D-galactose was measured as a sensitive indicator of cleft integrity (Table 2). The D-galactose equilibrium dissociation constant (K_D) revealed a significant perturbation for the C182/C95 di-cysteine protein, which yielded a K_D 5-fold greater than wild-type, indicating a significant decrease in sugar affinity. No significant changes in K_D were observed for the remaining six mutants, indicating that the effects of the engineered cysteines on sugar binding were generally minor (Table 2).

To probe for allosteric perturbations, the rate constant for Tb^{3+} dissociation from the calcium binding site, located 26 Å from the sugar binding cleft in the C-terminal domain, was measured (Table 2). Three of the seven engineered proteins, C182/C95, C182/C71, and C182/C26, exhibited minor perturbations: in each case the Tb^{3+} dissociation was slowed less than 0.3-fold, indicating that allosteric perturbation of calcium site dynamics were minimal. The remaining four engineered proteins exhibited Tb^{3+} dissociation kinetics that were the same, within error, as those measured for the native molecule (Table 2).

The ^{19}F NMR spectrum of 5-fluorotryptophan labeled GGBP provided an independent probe of both (i) perturbations within the substrate binding cleft, and (ii) allosteric effects (Luck & Falke, 1991b,c). This technique yields sensitive detection of structural changes in the vicinity of the five tryptophan positions in the molecule: W183, which lies in the cleft in van der Waals contact with the bound sugar; W284, located behind the cleft in the hinge region; W195, residing on an α-helix terminating in the sugar binding cleft; and W127 and W133, each lying within 10 Å of the calcium binding site. The ^{19}F NMR resonances of these five tryptophans are summarized in Table 3 for the wild-type and engineered proteins. Each engineered GGBP
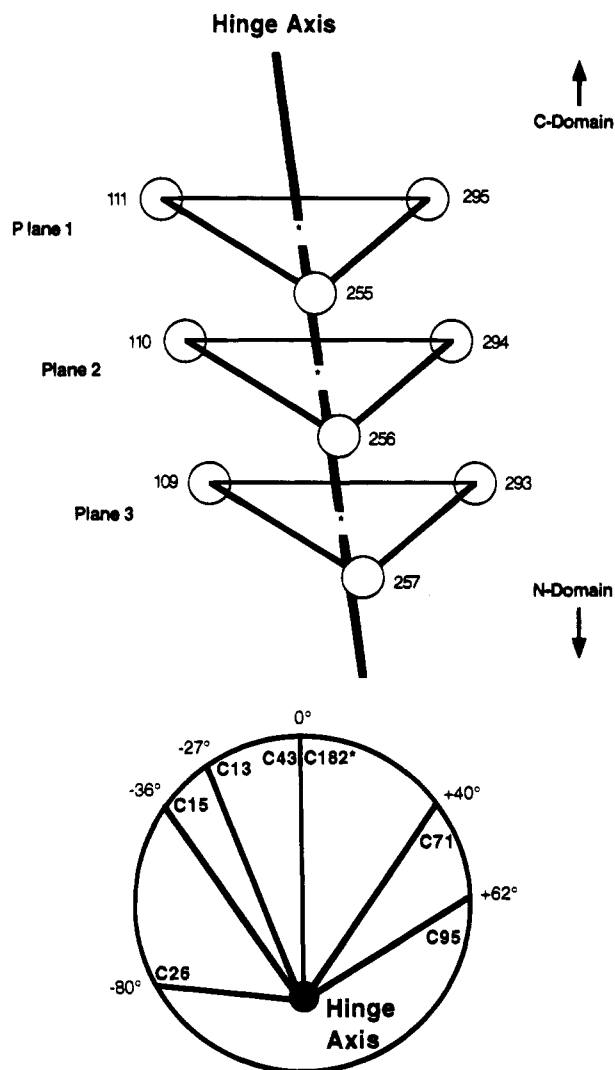
FIGURE 2: Definition of the hinge-twist motion. (A, top) Schematic drawing of the hinge axis defined by the three discontinuous hinge strands connecting the two domains. These hinge strands include the following residues: 109–111 (strand 1); 255–257 (strand 2); 293–295 (strand 3). Three planes can be drawn approximately parallel to the ligand binding cleft as shown, where each plane is defined by three α-carbons, one from each strand. The center of mass for the three α-carbons locates the intersection of their plane with the hinge axis. The best fit line connecting these three centers of mass defines the position of the hinge axis. (B, bottom) Schematic view down the hinge axis, looking from the N-terminal to the C-terminal domain. Illustrated are the angular positions of the engineered cysteines with respect to the hinge. Position 182, which provides the cysteine probe common to all the engineered cysteine pairs, is marked by the asterisk. The hinge-twist angle required to place position 182 over each other engineered cysteine postition is indicated. This hinge-twist motion causes one domain to rotate relative to the other, where the hinge axis defines the vertex of the twist angle. Position 43 lies directly below position 182 in the crystal structure; thus the C182/C43 cysteine pair defines the zero hinge-twist angle.

molecule exhibited resonances with chemical shifts and linewidths indistiguishable from those of the wild type, within the 0.1 ppm error of the measurement. Two of the mutants, C182/C71 and C182/C26, exhibited minor additional resonances not observed in the wild type, indicating that in both cases a small fraction of the protein population existed as a stable alternative conformer.

Further evidence regarding the integrity of the engineered GGBP proteins was provided by their successful overproduc-

Table 1: Positions Chosen for Cysteine Substitution

cysteine substitutions	twist angle $\Theta_T{}^a$ (deg)	C^β–C^β distance $r^\beta_{ij}{}^b$ (Å)	C^β solvent accessible surface area^c
M182C			37
M182C/Q26C	−80	(27.8)	37/47
M182C/D15C	−36	12.4	37/28
M182C/N13C	−27	12.3	37/80
M182C/N43C	0	8.9	37/50
M182C/A71C	40	15.9	37/88
M182C/S95C	62	21.1	37/63
M182C E240C		(18.4)	37/69

^{a} Hinge-twist angle, where the axis of rotation is defined in Figure 2 (see Results). ^{b} Distance between the β-carbons of the substituted positions. Values in parentheses indicate distances measured through the core of the protein, arising from a cysteine pair on opposite surfaces of the molecule. ^{c} For each substituted position the solvent-accessible surface area of the β-carbon was determined by first removing crystallographic waters and the distal atoms of the side chain. Subsequently the program ACCESS (Richards, 1977) was employed to calculate exposure to a 1.4 Å radius probe, with slab thickness 0.1 Å.

Table 2: Effect of Cysteine Substitutions on Ligand Affinity and Dissociation Rate

binding protein	D-galactose K_D $(\mu M)^a$	Tb^{3+} k_d $(\times\ 10^{-3}\ s^{-1}\ molecule^{-1})^b$
WT	0.3 ± 0.1	6.9 ± 0.7
M182C/D13C	0.1 ± 0.1	7.9 ± 0.9
M182C/N15C	0.3 ± 0.1	8.1 ± 0.9
M182C/Q26C	0.5 ± 0.1	5.7 ± 0.2
M182C/N43C	0.3 ± 0.1	8.1 ± 0.9
M182C/A71C	0.1 ± 0.1	4.7 ± 0.3
M182C/S95C	1.4 ± 0.8	5.8 ± 0.2
M182C/E240C	0.2 ± 0.1	6.1 ± 0.3

^{a} Dissociation constant for the D-galactose binding equilibrium, 25 °C. ^{b} Rate constant for Tb^{3+} dissociation from the Ca^{2+} binding site, 25 °C.

tion in *E. coli*. Since the GGBP molecule resides in the periplasmic compartment, where the bulk of the bacterial proteolytic enzymes are found, proteins with folding defects were not expected to accumulate. The seven di-cysteine GGBP molecules were each overproduced to approximately the same level as wild-type GGBP, indicating that they were all stable, well-folded proteins.

Together the data suggested that the engineered GGBP molecules were stable proteins in solution, providing useful systems in which to study hinge-twist motions. All of the di-cysteine proteins possessed multiple properties indistinguishable from those of wild type. The most native mutants were the C182/C15, C182/C43, and C182/C240 proteins, which were equivalent to wild type in all assays. Significantly, with the exception of the C182/C95 mutant, the engineered GGBP molecules each bound D-galactose with approximately the same affinity as wild type, suggesting normal function of the sugar binding cleft and hinge.

Detection of Internal Motions by Disulfide Trapping. Thermal motions yielded interdomain sulfhydryl–sulfhydryl collisions between the two cysteines in a given engineered molecule; these collisions were trapped and detected by oxidative disulfide formation. Disulfide formation reactions were triggered by the addition of the redox catalyst Cu^{2+}-(1,10-phenanthroline)$_3$ and used ambient dissolved oxygen as the oxidant (Kobashi, 1968; Careaga & Falke, 1992b). The oxygen–Cu^{2+}(1,10-phenanthroline)$_3$ system rapidly

Table 3: Effect of Cysteine Substitutions on 5-Fluorotryptophan ^{19}F NMR Resonances[a]

| binding protein | ^{19}F NMR chemical shift (uncertainty ±0.1 ppm) | | | | | | |
| | W127 | | W133 | | W183 | W195 | W284 |
	b	c	b	c			
WT	−46.0	−46.2	−51.2	−52.0	−42.9	−48.5	−52.5
M182C	−46.0	−46.2	−51.2	−51.9	−42.9	−48.4	−52.5
M182C/D13C	−46.0	−46.2	−51.2	−51.9	−42.8	−48.4	−52.5
M182C/N15C	−46.0	−46.2	−51.2	−51.9	−42.9	−48.4	−52.5
M182C/Q26C[d]	−45.7	−46.2	−51.3	−52.0	−43.1	−48.5	−52.5
M182C/N43C	−46.0	−46.2	−51.2	−51.9	−42.9	−48.4	−52.5
M182C/A71C[e]	−46.0	−46.2	−51.2	−51.9	−42.9	−48.4	−52.5
M182C/S95C	−46.0	−46.2	−51.2	−51.9	−42.9	−48.4	−52.5
M182C/E240C	−46.0	−46.2	−51.2	−51.9	−42.9	−48.4	−52.5

[a] ^{19}F NMR spectra of 5−fluorotryptophan labeled protein containing bound D-glucose and Ca^{2+} were obtained under reducing conditions at 25 °C, as described in Materials and Methods. [b,c] Residues W127 and W133, which are in VDW contact with one another near the Ca^{2+} site, each detect two stable conformers of their local environment, as previously discussed (Luck & Falke, 199a,b). [d] The spectrum of double mutant M182C/Q26C exhibited two resonances for W183: one at the normal frequency (−43.1 ppm, 60%) and one at a different frequency (−47.2 ppm, 40%). Thus two stable conformers were present. The single mutant M182C exhibited only the normal frequency. [e] The spectrum of M182C/A71C exhibited two additional minor resonances (−49.7, −42.6 ppm) which indicated the presence of multiple stable conformers.

produces oxyradicals (hydroxyl radical or superoxide anion) capable of diffusing to the site of sulfhydryl oxidation (Oae, 1991; Snyder, 1987; Bull et al., 1983; Cecil et al., 1959). The resulting oxidation chemistry yields two competing reactions:

$$RSH + RSH \xrightarrow[O_2, Cu(phen)_3]{k_{SS}} RS-SR$$

$$RSH \downarrow k_2 \quad O_2, Cu(phen)_3$$

$$RSH + RX$$
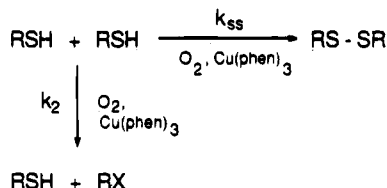
where both the intended disulfide bond product (R-S-S-R′) and undesired higher oxidation products of cysteine (the sulfinic acid R-SO$_2^-$, and the sulfonic acid R-SO$_3^-$) are generated.

To separate reaction products containing an intramolecular disulfide from those lacking disulfides, the products of the oxidation reaction were subjected to electrophoresis on a nonreducing SDS/polyacrylamide gel. Resolution of products resulted from the higher mobility of the disulfide-containing molecule, which was more compact due to its intramolecular cross-link (Goldenberg & Creighton, 1984; Falke et al., 1988; Careaga & Falke, 1992b). In each case this increased mobility was reversed by reduction, verifying that it stemmed from a disulfide bond. The rate constants of the disulfide formation reaction (k_{SS}) and the competing sulfhydryl oxidation (k_2) were determined by best fit of a two-component reaction scheme to the observed reaction time course (Careaga & Falke, 1992b):

$$F_{SS}(t) = \frac{k_{SS}}{k_{SS} + k_2}[1 - e^{-(k_{SS}+k_2)}] \qquad (2)$$

where $F_{SS}(t)$ is the fraction of the di-cysteine receptor population containing an intramolecular disulfide bond, and

the two reactions are defined in eq 1 above. The resulting kinetic parameters are summarized in Table 4.

The interpretation of disulfide formation rate data was facilitated by quantitating the intrinsic chemical reactivity of each engineered cysteine, as operationally defined by the rate of alkylation with [^{14}C]iodoacetamide. This alkylation reaction was expected to be sensitive to structural, dynamic, and electrostatic parameters similar to those controlling reactivity in oxidation reactions: to be either alkylated or oxidized, an engineered sulfhydryl must (i) be converted to the sulfanion by deprotonation and then (ii) collide with a small molecule alkylation reagent or oxidant, respectively. As summarized in Table 4, the engineered GGBP molecules exhibited less than a 4-fold range of iodoacetamide labeling rates.

Disulfide-Trapped Motions in the D-Glucose Occupied Binding Protein. The disulfide trapping approach revealed large domain rotations in GGBP even when the ligand binding cleft contained bound D-glucose. Counterclockwise hinge twisting motions ranging from −36° to 0° were detected as three disulfide-trapped products: C182−C43 (0°); C182−C13 (−27°); and C182−C15 (−36°), (Table 4). These trapped motions did not stem from global unfolding of the protein, since no disulfide-trapped products were observed for the four remaining engineered molecules probing the most extreme counterclockwise twist (C182/C26), the clockwise twists (C182/C71, C182/C95), and unfolding of the C-terminal domain (C182/C240). Instead the disulfide-trapped products were consistent with a simple hinge-twisting motion of two stably folded domains.

The rate of disulfide bond formation provided information concerning the frequency of hinge-twisting in the D-glucose occupied cleft. Disulfide formation rates were observed to vary over a ≥430-fold range (Table 4). As expected, the most proximal cysteine pair (C182/C43) exhibited the most rapid disulfide formation kinetics, suggesting that it possessed the highest collision rate. Differences in the intrinsic reactivities of cysteines did not account for this large range of disulfide formation rates: the competing oxidation reaction (k_2) exhibited only a 16-fold kinetic range, while the iodoacetamide reactivity varied only 4-fold (k_{IA}, see above and Table 4). Moreover, the relative disulfide formation rates of different cysteine pairs exhibited a strong correlation with their angular hinge-twist proximity, while little correlation was observed with their chemical reactivities (Table 4). These results reinforce the previous conclusion (Careaga & Falke, 1992b) that, for surface cysteines, the disulfide formation rate is controlled primarily by the rate of sulfhydryl−sulfhydryl collisions, rather than by the reactivity of individual cysteine residues.

Disulfide-Trapped Motions in the Sugar-Empty Protein. When sugar was removed from the cleft, two additional engineered cysteine pairs yielded detectable disulfide bond formation: C182−C26 (−80°) and C182−C71 (+40°). These disulfides extended the detected motional range in both the counterclockwise and clockwise directions (Table 4). Disulfide formation rates were also observed to increase for five of the seven engineered Cys pairs, from a 2.5-fold rate increase for the C182−C13 formation reaction to a minimum 700-fold increase for C182−C26 formation. Thus removal of ligand generated both larger motional amplitudes and more rapid kinetics for the hinge twist motions.

Table 4: Sulfhydryl Reactivity and Disulfide Formation Rate Constants[a]

cysteine pair	Θ_T (deg)	k_{IA} (s^{-1} M^{-1})	(+) D-glucose			(−) D-glucose		
			k_{SS} (× 10^{-3} s^{-1} molecule^{-1})	k_2	$F_{SS}(\infty)$	k_{SS} (× 10^{-3} s^{-1} molecule^{-1})	k_2	$F_{SS}(\infty)$
182/26	−80	1.8 ± 0.2	~0[b]		~0	14 ± 3	20 ± 10	0.36
182/15	−36	3.3 ± 0.2	0.13 ± 0.06	1.1 ± 0.6	0.11	9 ± 1	15 ± 2	0.37
182/13	−27	5.9 ± 0.3	2.8 ± 0.3	5.7 ± 0.7	0.34	7 ± 1	6 ± 1	0.54
182/43	0	2.1 ± 0.1	9 ± 2	18 ± 5	0.32	35 ± 3	55 ± 7	0.40
182/71	+40	1.5 ± 0.1	~0[b]		~0	2 ± 1	4 ± 3	0.33
182/95	+62	6.0 ± 0.3	~0[b]		~0	~0[b]		~0
182/240		2.4 ± 0.1	~0[b]		~0	~0[b]		~0

[a] All reactions were carried out at 37 °C as described in Materials and Methods. Θ_T = amplitude of hinge-twist angle defined by engineered cysteines. k_{IA} = pseudo-first-order rate constant for reaction with 1.0 × 10^{-4} M [^{14}C]iodoacetamide. k_{SS} = pseudo-first-order rate constant for intramolecular disulfide formation in the standard oxidation reaction. k_2 = pseudo-first-order rate constant for the competing formation of higher sulfhydryl oxidation products in the standard oxidation reaction. F_{SS} = fractional disulfide formation at completion of the reaction, calculated as $F_{SS}(\infty) = k_{SS}(k_{SS} + k_2)^{-1}$, where a value less than unity indicates the formation of higher sulfhydryl oxidation products. [b] No disulfide formation detected over the course of a 5 h reaction. The absence of an observable reaction time course precluded measurement of the competing higher oxidation reaction. For the 182/71 and 182/95 proteins in the absence of D-glucose, a small population of disulfide containing products [$F_{SS}(\infty) \leq$ 0.1] was observed to form before the first time point, but no further reaction occurred during the time course. This minor population was assumed to represent denatured protein generated during sugar removal.

Table 5: Estimated Amplitudes and Frequencies of Observed Intramolecular Motions[a]

cysteine pair	twist angle	minimum translation		minimum rotation			rate constant (per molecule)			
							(+) D-glucose		(−) D-glucose	
	Θ_T (deg)	r^β_{ij} (Å)	Δr^β_{ij} (Å)	$\Delta\chi^\beta_{ij}$ (deg)	$\Delta\theta_{ij}$ (deg)	$\Delta\theta_{ji}$ (deg)	k_{SS} (×10^{-3} s^{-1})	k_C (s^{-1})	k_{SS} (×10^{-3} s^{-1})	k_C (s^{-1})
182/26	−80	(27.8)	23.2	143	99	73	~1	<1	14 ± 3	~10^3
182/15	−36	12.4	7.8	122	66	90	0.13 ± 0.06	~10^1	9 ± 1	~10^3
182/13	−27	12.3	7.7	43	102	86	2.8 ± 0.3	~10^2	7 ± 1	~10^3
182/43	0	8.9	4.3	51	124	140	9 ± 2	~10^3	35 ± 3	~10^3
182/71	40	15.9	11.3	−70	88	102	~0	<1	≤2 ± 1	≤10^2
182/95	62	21.1	16.5	−49	70	79	~0	<1	~0	<1
182/240		(18.4)	13.8	2	63	137	~0	<1	~0	<1

[a] Θ_T = amplitude of hinge-twist angle defined by engineered cysteines. r^β_{ij} = distance between β-carbons of the two engineered cysteines. Δr^β_{ij} = minimum relative translation required to bring the cysteine β-carbons into disulfide formation range (Careaga & Falke, 1992b). $\Delta\chi^\beta_{ij}$ = minimum rotation of pseudo-dihedral angle required to bring cysteines into disulfide formation geometry (Careaga & Falke, 1992b). $\Delta\theta_{ij}$ = minimum rotation of pseudo-bond angle required to bring cysteines into disulfide formation geometry (Careaga & Falke, 1992b). k_{SS} = pseudo-first-order rate constant for intramolecular disulfide formation in the standard oxidation reaction, 37 °C. k_C = rate constant of intramolecular sulfhydryl−sulfhydryl collisions at 37 °C estimated from the relationship $k_{SS} = \sigma k_C$, where the efficiency of disulfide formation in the standard oxidation reaction is $\sigma \sim 10^{-5}$ (Careaga & Falke, 1992b).

DISCUSSION

To use disulfide trapping as a probe of hinge twist motions in the sugar binding cleft, it was necessary to engineer di-cysteine proteins which were stable and unperturbed in assays sensitive to protein folding and dynamics. Each of the seven di-cysteine proteins produced for this study was observed to be well expressed and stable folded. Moreover, with the exception of C182/C71 and C182/C95, each di-cysteine protein exhibited multiple properties identical to native GBP in analyses which quantitated ligand binding affinity, ligand dissociation kinetics, and ^{19}F NMR spectral parameters. The minor perturbations observed for the C182/C71 and C182/C95 proteins did not significantly destabilize their structures, since they remained proteolytically resistant and did not exhibit rapid intramolecular disulfide formation, the latter being a feature of unfolded protein (Careaga & Falke, 1992b). Thus, each of the di-cysteine GBP molecules were useful probes of conformational dynamics.

Disulfide trapping studies utilizing these engineered cysteine pairs revealed intramolecular collisions between pairs of engineered cysteines in different structural domains, resulting from previously undetected large amplitude thermal motions. The simplest type of trajectory capable of generating proximity between the engineered cysteines is a hinge twist motion, in which the C-terminal and N-terminal

domains undergo relative rotations about an axis parallel to the three hinge strands connecting the two domains. Table 5 summarizes the hinge twist angle required for closest approach of each cysteine pair, ranging from a counterclockwise motion of −80° (for the C182/C26 pair) to a clockwise rotation of +62° (for C182/C95). Also tabulated are the minimum translational and rotational motions required to bring each cysteine pair into a geometry compatible with disulfide formation, calculated as detailed in a previous application of the disulfide trapping approach (Careaga & Falke, 1992b).

When the ligand binding cleft between the two domains is occupied by D-glucose, the hinge twist is limited to counterclockwise rotations ranging between 0° and −36°, which are trapped by disulfide bonds C182−C43 (0°), C182−C13 (−27°), and C182−C15 (−36°). Not surprisingly, the disulfide formation rate is 66-fold higher for the collision requiring no hinge twist (0°) than for the collision requiring the largest counterclockwise twist (−36°). When sugar is removed from the cleft, both the amplitude and frequency of hinge twist motions increase substantially: the range of motion becomes −80° to +40°, and the rate of disulfide formation increases up to 700-fold. The most rapid reaction is still observed for the collision requiring no hinge twist, which is at least 17-fold faster than the extreme

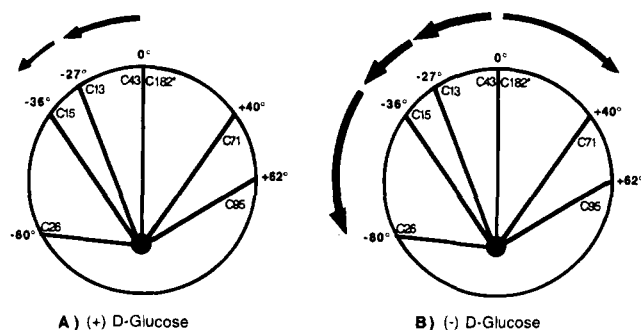**A) (+) D-Glucose**   **B) (-) D-Glucose**

FIGURE 3: Schematic summary of observed hinge twist motions. The hinge-twist motions detected by disulfide trapping are indicated by curved arrows. The width of the arrows represents the relative frequencies of their respective hinge twist motions (see Table 5).

clockwise rotation trapped by the disulfide bond C182—C71 (+40°). The observed ranges and relative frequencies of hinge-twist motions are schematically illustrated in Figure 3.

It should be noted that the collisions detected by disulfide trapping may require both the hinge-twist motion and transient unfolding of small regions of one or both domains. Such local unfolding could help generate the local geometry required for disulfide formation. However the hinge twist, rather than unfolding, provides the bulk of the motion responsible for the observed collisions, as evidenced by four factors. (i) The measured disulfide formation rates are correlated more strongly with hinge-twist angle than any other motional parameter. For example, the C_β–C_β distance for the C182/C13 and C182/C15 pairs are virtually identical (12.3 vs 12.4 Å, respectively); however, the former pair forms a disulfide 20-fold more rapidly in the D-glucose occupied protein, consistent with its smaller hinge twist angle (−27° vs −36°, respectively). (ii) Extensive unfolding reactions in either domain are inconsistent with the observed stability of the engineered proteins in the periplasmic compartment, which contains high protease concentrations. (iii) The control pair C182/C240, in which both cysteines lie in the C-terminal domain, exhibits no detectable disulfide formation unless the protein is first unfolded with urea, indicating that extensive unfolding of the C-domain does not occur until denaturation. (iv) With the exception of C26 and C240, each of the engineered cysteines lies on a loop bridging a β-strand to an α-helix, where the β-strand is firmly anchored in the β-sheet at the core of the domain. Thus extensive local motion of the loop would require unfolding of the protein core.

For a given pair of cysteines, the observed rate of disulfide formation provides insight into the time scale of the motions detected by disulfide trapping. The disulfide formation rate constant (k_{SS}) can be converted into a sulfhydryl—sulfhydryl collision rate constant (k_C) using a simple linear relationship (Careaga & Falke, 1992b):

$$k_{SS} = \sigma k_C \qquad (3)$$

where the proportionality constant (σ) represents the efficiency factor of the disulfide reaction. For two cysteines on the surface of a protein reacting under the specified oxidation conditions, the efficiency factor has been estimated to be $\sigma \sim 10^{-5}$, indicating that only one in 10^5 collisions will result in disulfide formation (Careaga & Falke, 1992b). The estimated collision rates obtained using this efficiency

factor are summarized in Table 5. When D-glucose is bound in the cleft, the sulfhydryl—sulfhydryl collision rate ranges over two orders of magnitude (from 10^3 to 10^2 to 10^1 s^{-1} for the 0°, the −27°, and the −36° twist angles, respectively). Since a sugar molecule typically resides in the cleft for a period of 0.5 s (Miller et al., 1983), the estimated collision rates require that the −27° hinge twist occurs roughly 50 times before the sugar is released, while the −36° hinge twist occurs approximately five times during the bound sugar lifetime. When the cleft is empty, the observed hinge twisting rates are more similar, indicating that the energy barrier for twisting becomes less steep.

Overall, the disulfide trapping and NMR results presented here and elsewhere suggest the following model for motions of the sugar binding cleft in solution. The interdomain hinge possesses at least two degrees of rotational freedom. NMR studies reveal that the hinge can bend, enabling the sugar binding cleft to open by at least 18° (Luck & Falke, 1991a). The present disulfide trapping results indicate that the hinge can also twist, yielding twist angles spanning a 36° range when sugar is bound in the cleft or a 120° range when the cleft is empty. The hinge-twist motion requires the two cleft surfaces to slide relative to one another. One feature of the cleft structure which may facilitate this sliding is the presence of a layer of water molecules between the cleft surfaces (Vyas et al., 1987); this solvent layer prevents extensive direct contacts between the two domains and could act as a molecular lubricant. Another feature likely required for hinge twisting is extensive mobility of the hinge strands. Evidence that such mobility indeed exists has been provided by an earlier disulfide trapping study, which revealed up to 15 Å relative motions of the helix $\alpha 10$ contiguous with the third hinge strand (Careaga & Falke, 1992b). The lower collision rates observed for clockwise twisting motions may stem from the shape of the cleft rim within the N-terminal domain, which slopes away from the C-terminal rim in the region sampled by clockwise rotations. As a result, collisions in this region would require more extensive hinge bending or local unfolding as well as the hinge twist.

What are the biological functions of the observed hinge motions? Hinge bending is certainly required for ligand binding and release, since the structure of the D-glucose occupied cleft completely engulfs the bound sugar. A sugar molecule can neither enter nor leave this closed conformation of the cleft unless it opens via a hinge bend. The function of hinge twisting is less obvious, but it could play an essential role in the regulation of binding protein docking to its membrane targets. GBP is involved in both chemotaxis and sugar transport, where the sugar-occupied conformer docks to a a transmembrane receptor or transport protein, respectively. The membrane-bound components must thus be able to discriminate between the sugar-occupied and apo-states of the protein. This discrimination must be quite efficient, especially considering the high concentration of the binding protein (∼1 mM) in the periplasmic compartment (Neidhart, 1987). Mutational studies of periplasmic binding proteins have revealed a receptor docking surface spanning the entrance to the interdomain cleft (Spurlino et al., 1991; Gardina et al., 1992). An apo-state exhibiting hinge twisting motions as well as hinge bending could more effectively disrupt this docking surface, thereby ensuring that the inactive protein does not compete with the ligand-occupied protein for membrane binding.

The hinge twisting motions observed in GBP possess the largest amplitudes seen to date for motions of this type, ranging from 36° with ligand bound to 120° for the apo-cleft. Crystallographic studies of citrate synthase and the maltose binding protein have revealed smaller hinge twists of 18° and 8°, respectively (Lesk & Chothia, 1984; Sharff et al., 1992), but the present results raise the possibility that such proteins may exhibit larger domain twisting motions in solution. Large amplitude hinge bending motions have been observed in a wider array of proteins, including adenylate cyclase (88°; Berry et al., 1994), lysine/arginine/ornithine binding protein (52°; Oh et al., 1993), maltose binding protein (35°; Sharff et al., 1992), lysozyme (32°; Faber & Matthews, 1990), and galactose binding protein (≥18°; Luck & Falke, 1991a). Together these observations contribute to the dynamic description of protein structure [reviewed in Straatsma and McCammon (1992), Karplus (1986), and Gertstein et al. (1994)] in which large amplitude motions of the polypeptide backbone and entire domains can play functionally important roles on biologically relevant time scales.

ACKNOWLEDGMENT

REFERENCES

Bennett, W. S., & Steitz, T. A. (1980) *J. Mol. Biol. 140*, 211−230.

Bennett, W. S., & Huber, R. (1984) *Crit. Rev. Biochem. 15*, 291−384.

Berry, M. B., Meador, B., Bilderback, T., Liang, P., Glaser, M., & Phillips, G. N., Jr. (1994) *Proteins: Struct., Funct., Genet. 19*, 183−198.

Bull, C., McClune, G. J., & Fee, J. A. (1983) *J. Am. Chem. Soc. 105*, 5290−5300.

Careaga, C. L., & Falke, J. J. (1992a) *Biophys. J. 62*, 209−219.

Careaga, C. L., & Falke, J. J. (1992b) *J. Mol. Biol. 226*, 1219−1235.

Cecil, R., & McPhee, J. R. (1959) *Adv. Protein Chem. 14*, 255−389.

Dixon, M. M., Nicholson, H., Shewchuk, L., Baase, W. A., & Matthews, B. W. (1992) *J. Mol. Biol. 227*, 917−934.

Eklund, H., Samma, J. P., Wallen, L., Branden, C. I., Akeson, A., & Jones, T. A. (1981) *J. Mol. Biol. 146*, 561−587.

Faber, H. R., & Matthews, B. W. (1990) *Nature 348*, 263−265.

Falke, J. J., & Koshland, D. E., Jr. (1987) *Science 237*, 1596−1600.

Falke, J. J., Dernberg, A. F., Sternberg, K. A., Zilkin, N., Milligan, D. L., & Koshland, D. E., Jr. (1988) *J. Biol. Chem. 263*, 14850−14858.

Gardina, P., Conway, C., Kossman, M., & Manson, M., (1992) *J. Bacteriol. 174*, 1528−1536.

Gerstein, M., Lesk, A. M., Baker, E. N., Anderson, B., Norris, G., & Chothia, C. (1993) *J. Mol. Biol. 234*, 357−376.

Gerstein, M., Lesk, A. M., & Chothia (1994) *Biochemistry 33*, 6739−6749.

Goldenberg, D. P., & Creighton, T. E. (1984) *Anal. Biochem. 138*, 1−18.

Karplus, M. (1986) *Methods. Enzymol. 131*, 283−307.

Karlsson, R., Zheng, J. H., Xuong, N. H., Taylor, S. S., & Sowadski, J. M. (1993) *Acta Crystallogr. D49*, 381−395.

Kobashi, K. (1968) *Biochim. Biophys. Acta 158*, 239−245.

Kunkel, T. A., Roberts, J. D., & Zakour, R. A. (1988) *Methods Enzymol. 154*, 367−382.

Laemmli, U. K. (1979) *Nature 227*, 680−685.

Lesk, A. M., & Chothia, C. (1984) *J. Mol. Biol. 174*, 175−191.

Luck, L. A., & Falke, J. J. (1991a) *Biochemistry 30*, 6484−6490.

Luck, L. A., & Falke, J. J. (1991b) *Bioichemistry 30*, 4248−4256.

Luck, L. A., & Falke, J. J. (1991c) *Biochemistry 30*, 4257−4261.

Miller, D. M., Olson, J. S., Plugrath, J. W., & Quiocho, F. A. (1983) *J. Biol. Chem. 258*, 13665−13672.

Muller, N., Heire, H. G., & Boos, W. (1985) *J. Bacteriol. 163*, 37−45.

Neidhart, F. C. (1987) in *E. coli and S. typhimurium, Cellular and Molecular Biology*, pp 1−6, 56−69, and 732−759, American Society of Microbiology, Washington, D.C.

Oae, S. (1991) in *Organic Sulfur Chemistry: Structure and Mechanism* (Doi, J. T., Ed.), pp 203−281, CRC Press, Boca Raton, FL.

Oh, B.-H., Pandit, J., Kang, C.-H., Nikaido, K., Gokcen, S., Ames, G. F.-L., & Kim, S.-H. (1993) *J. Biol. Chem. 268*, 11348−11359.

Quicho, F. A., Vyas, N. G., Sack, J. S., & Vyas, M. N. (1987) *Cold Spring Harbor Symp. Quant. Biol.. 52*, 453−463.

Richards, F. M. (1977) *Annu. Rev. Biophys. Bioeng. 6*, 151−176.

Sharff, A. J., Rodseth, L., Spurlino, J. C., & Quiocho, F. A. (1992) *Biochemistry 31*, 10657−10671.

Snyder, G. H. (1987) *Biochemistry 26*, 688−694.

Spurlino, J. C., Lu, G. Y., & Quiocho, F. A. (1991) *J. Biol. Chem. 266*, 5202−5219.

Stillman, T. J., Baker, B. J., Britton, K. L., & Rice, D. W. (1993) *J. Mol. Biol. 234*, 1131−1149.

Straatsma, T. P., & McCammon, J. A. (1992) *Annu. Rev. Phys. Chem. 43*, 407−435.

Vyas, N. K., Vyas, M. N., & Quiocho, F. A. (1987) *Nature 327*, 635−638.

Weber, I. T., & Steitz, T. A. (1987) *J. Mol. Biol. 198*, 311−323.

Zahler, W. L., & Cleland, W. W. (1968) *J. Biol. Chem. 243*, 716−719.

Zou, J. Y., Flocco, M. M., & Mowbray, S. M. (1993) *J. Mol. Biol. 233*, 739−752.